PNAS RESEARCH ARTICLE | APPLIED PHYSICAL SCIENCES

Digital rheometer twins: Learning the hidden rheology of complex fluids through rheology-informed graph neural networks

Mohammadamin Mahmoudabadbozchelou[a], Krutarth M. Kamani[b], Simon A. Rogers[b], and Safa Jamali[a,1]

Edited by David Weitz, Harvard University, Cambridge, MA; received February 7, 2022; accepted March 28, 2022

Precise and reliable prediction of soft and structured materials' behavior under flowing conditions is of great interest to academics and industrial researchers alike. The classical route to achieving this goal is to construct constitutive relations that, through simplifying assumptions, approximate the time- and rate-dependent stress response of a complex fluid to an imposed deformation. The parameters of these simplified models are then identified by suitable rheological testing. The accuracy of each model is limited by the assumptions made in its construction, and, to a lesser extent, the ability to determine numerical values of parameters from the experimental data. In this work, we leverage advances in machine learning methodologies to construct rheology-informed graph neural networks (RhiGNets) that are capable of learning the hidden rheology of a complex fluid through a limited number of experiments. A multifidelity approach is then taken to combine limited additional experimental data with the RhiGNet predictions to develop "digital rheometers" that can be used in place of a physical instrument.

physics-informed neural networks | rheology | rheology-based machine learning | data-driven constitutive modeling

Significance

Science-based data-driven methods that can describe the rheological behavior of complex fluids can be transformative across many disciplines. Digital rheometer twins, which are developed here, can significantly reduce the cost, time, and energy required to characterize complex fluids and predict their future behavior. This is made possible by combining two different methods of informing neural networks with the rheological underpinnings of a system, resulting in quantitative recovery of a gel's response to different flow protocols. The platform developed here is general enough that it can be extended to areas well beyond complex fluids modeling.

The quest to accurately predict the rheology of a complex fluid is as old as our ability to synthesize and measure it. For over a century, phenomenological models have been developed to describe the stress response of a complex fluid to an applied deformation. Generally, the number of model parameters and the complexity of the model grow with the complexity of the fluid's response to a particular flow. For instance, embedding the time-dependent response of a thixotropic elastoviscoplastic fluid into a constitutive equation commonly requires additional equations to be coupled with the main stress–strain calculator. As a result, rheological constitutive equations for complex fluids are often described through a series of coupled ordinary or partial differential equations. Many challenges exist in predicting the rheology of complex fluids through these equations. One challenge is that, since these models are often developed from the perspective of fundamental and phenomenological components that describe a material, such as dashpots, springs, and sliding blocks, they do not necessarily predict the rheological response of a complex multicomponent system accurately. Another challenge is that, as the number of equations and material constants grows, the number of experiments required to characterize them increases as well. A third challenge, which may be the most important, is that these predictions do not evolve as one's understanding of the material does. In other words, once the differential equations have been set, and their parameters determined, there are no mechanisms by which improved predictions can be made. However, these constitutive models are mathematical manifestations of the underlying physical laws that govern the rheology of the material and are demonstrated in the experimental results. A more efficient path would allow for the continual evolution of predictions as limited experimental data are obtained. Such methodologies can be transformative as novel material characterization techniques.

Data-driven models have become incredibly powerful tools for analyzing and predicting various phenomena (1–4), owing to ever-increasing computational power and the ability to process a large amount of data at an extraordinary rate. Machine learning (ML) techniques have been employed in virtually all avenues of science and engineering, and myriad different methodologies have emerged. Despite their widespread use, conventional ML frameworks are purely statistical in their foundation and rely on an abundance of data to achieve accuracy in their predictions. This implies that most ML algorithms are constrained to predictions in the range of data used in their training (interpolation), and are generally incapable of making out-of-range predictions (extrapolation). Recent advances in physics-based ML algorithms have alleviated such issues by directly integrating physical governing laws into the training process. Physics-informed neural networks (NNs) (5) provide a platform for the inclusion of the physical underpinnings of a system

Author affiliations: [a]Department of Mechanical and Industrial Engineering, Northeastern University, Boston, MA 02115; and [b]Department of Chemical and Biomolecular Engineering, University of Illinois Urbana–Champaign, Champaign, IL 61801

Author contributions: S.A.R. and S.J. designed research; M.M. and K.M.K. performed research; M.M., S.A.R., and S.J. analyzed data; and M.M., K.M.K., S.A.R., and S.J. wrote the paper.

The authors declare no competing interest.

This article is a PNAS Direct Submission.

[1]To whom correspondence may be addressed. Email: s.jamali@northeastern.edu.

Published May 11, 2022.

into the ML algorithm. These physical laws can be included implicitly or explicitly into the NN (6, 7). The explicit incorporation of the governing physical laws in the form of differential equations has been shown to be particularly effective in speeding up the solution of problems involving well-established constitutive models (8–12). In contrast, when the physical principles governing the problem are not particularly accurate, implicit incorporation of physics through data itself can be more beneficial. By assimilating the core physics of the problem, large training datasets are made redundant.

Rheology-informed NNs can be devised by informing the ML platform of the underlying rheological constitutive models both implicitly (13) and explicitly (14). These NNs can also be integrated with conservation laws into computational fluid dynamics, and solved to provide velocity fields and fully resolved flow fields for complex fluids under different flows (15). In this study, we present a graph-based NN that effectively and accurately learns the hidden rheology of a complex fluid with respect to multivariant constitutive equations, using a limited number of simple flow protocols. We then use this rheology-informed graph NN (RhiGNet) to predict other rheological features of the test material on flows that have not been used in the training. Ultimately, by combining the observational and the inductive learning features, a digital rheometer twin is devised. We show that this digital rheometer twin is capable of precisely measuring the complex response of a fluid to different flow protocols with unprecedented accuracy. This is beyond what has been made possible with any constitutive model regardless of model's type or foundation.

Materials and Methods

We study a thixotropic fluid (16, 17) that is a fumed silica colloidal suspension, which consists of a hydrophobic fumed silica (R972, Evonik), a highly refined paraffin oil (18512, Sigma-Aldrich), and a low molecular weight polybutene (H25, Indopol). The fumed silica, at 2.9 vol%, was dispersed in paraffin oil and large molecular weight polyisobutylene, with the ratio between them being 69 wt%:31 wt%. The sample was mixed with a Thinky mixer running at 2,000 rpm for 1 h. All measurements are performed with the same batch of this suspension.

The rheological experiments were carried out on an ARES-G2, a strain-controlled rheometer produced by TA Instruments, at 20 °C by using a cone and plate geometry (diameter, 40 mm; cone angle, 2° [part no. 402760.901]). All rheological properties were collected via TRIOS software. Before performing any measurements, the material was presheared using a protocol described by Choi and Rogers (18), which consists of three steps. In the first step, a shear rate of 200 s^{-1} is applied for 300 s. Immediately following shear cessation, a strain of 80% is applied in the direction opposite to the high shear-rate step to eliminate any directional bias produced from the high-rate shearing. The material is then held at 0 s^{-1} for 500 s to allow for the rebuilding of the isotropic structure.

Thixotropic Constitutive Models. The time-dependent stress response of complex fluids originates from their inherent viscoelastic and/or thixotropic properties. Thixotropy refers to the sensitivity of the stress response to the history of the applied deformation (19–21) and emerges in fluids whose microstructure evolves under flow due to a consistent competition between structure build-up and break-up. Many constitutive models have been proposed to recover this competition through a time evolution equation written for a scalar microstructure parameter. Nonetheless, the choice of constitutive model should be also made considering the thermodynamic consistency of the model's prediction with regard to different flow protocols and conditions. Otherwise, integration of inconsistent constitutive models into the NN can result in erroneous results for other flow protocols outside the range of experimental observations. A number of constitutive models can be adapted to recover the generic form of the rheological features observed in the fumed silica gel studied here. In this work, and to fully capture the response of a complex thixotropic-elasto-visco-plastic fluid, the Bauschinger effect and kinematic hardening are embedded in the plastic component of the model. The isokinematic hardening (IKH) model (22, 23) decouples the applied shear strain into plastic and viscoelastic contributions, while introducing a back strain to account for the microstructure orientation with respect to the direction of flow. The general form of the IKH model can be written as a set of Eqs. **1**, where γ_{ve} and γ_p are the viscoelastic and plastic component of the applied shear strain, G is the elastic modulus, η_v and μ_p are viscoelastic and plastic viscosities, A is the back strain, C is the back stress modulus, m and q are unitless material constants, k_3 is a material constant with unit of stress, and k_1 and k_2 are the build-up and breakage coefficients of the structure parameter.

$$\begin{cases} \gamma(t) = \gamma_{ve}(t) + \gamma_p(t) \\ \dot{\gamma}_{ve}(t) = f(\sigma, G, \eta_v, \gamma_{ve}(t)) \\ \dot{\gamma}_p(t) = \frac{1}{\mu_p} sign(\sigma - CA(t)) max(0, |\sigma - CA(t)| - k_3\lambda(t)). \\ \dot{A}(t) = \dot{\gamma}_p - (q|A(t)|)^m sign(A(t))|\dot{\gamma}_p(t)| \\ \dot{\lambda}(t) = k_1(1 - \lambda(t)) - k_2\lambda(t)|\dot{\gamma}_p(t)| \end{cases} \quad [1]$$

The function $f(.)$ is determined based on the viscoelastic model of choice that leads to the acquisition of various models, that is, Maxwell IKH (MIKH), Kelvin IKH, and Elastic IKH. Here we adapt an MIKH model to describe the rheology of fumed silica gels, as shown in Eq. **2** with nine (9) model parameters.

$$\begin{cases} \gamma(t) = \gamma_{ve}(t) + \gamma_p(t) \\ \dot{\gamma}_{ve}(t) = \frac{1}{G}\dot{\sigma} + \frac{1}{\eta_v}\sigma \\ \dot{\gamma}_p(t) = \frac{1}{\mu_p} sign(\sigma - CA(t)) max(0, |\sigma - CA(t)| - k_3\lambda(t)). \\ \dot{A}(t) = \dot{\gamma}_p - (q|A(t)|)^m sign(A(t))|\dot{\gamma}_p(t)| \\ \dot{\lambda}(t) = k_1(1 - \lambda(t)) - k_2\lambda(t)|\dot{\gamma}_p(t)| \end{cases} \quad [2]$$

Physics-Informed NNs. There are two main categories of ML frameworks. These are referred to as supervised learning and unsupervised learning (24). NNs are a subset of ML techniques that create a computational data-driven framework to reconcile the intricate relation between inputs and outputs. This is achieved by adjusting the variables of each neuron to reduce the deviations between the actual and predicted data. Traditional NN training processes are carried out solely on a statistical basis. This has proven to be effective and accurate when extremely large amounts of data are available and can be used for training the NN. However, such data simply do not exist in many engineering/scientific applications. For these cases, one can account for insufficient training data by incorporating the physical laws of interest into the NN architecture directly (5). These physical underpinnings can be injected into the NN through three different pathways: observational biases, learning biases, and inductive biases. Observational biases refer to the inclusion of the physics in the observed data, which results in implicit enforcement of physics during the training process (13, 25). Learning biases can be softly penalized to favor of a specific solution or physical law (26, 27), resulting in so-called physics-guided NNs. Alternatively, one can incorporate the physical laws of interest in the form of differential equations into the architecture of the NN, imposing a hard penalty (14, 28–30) and construction of physics-informed NNs. While different in methodology, these pathways are not necessarily exclusive and can be used simultaneously.

Here, we first introduce an inductive bias method, RhiGNet, using the foundations in the ADCME library (Automatic Differentiation Library for Computational and Mathematical Engineering) (31) that are tailored to rheology-related applications. The backend of ADCME is TensorFlow, a high-performance deep learning framework that offers parallel processing and automatic differentiation based on computational graphs, in which a value is represented as an edge, and a node represents a function. In an inverse RhiGNet framework, we use a very limited number of experimental data to recover all the parameters of the MIKH model (Eq. **2**). The input data of RhiGNet are an $n \times 3$ matrix, consisting of time, imposed shear rate, $\dot{\gamma}$, and the shear stress, σ, measured experimentally. Using these experimental measurements, RhiGNet minimizes the residual for the constitutive model of choice, in this case the MIKH, and returns the predicted model parameters. The variables of an inverse RhiGNet framework are trained by minimizing the loss function defined in Eq. **3**, including the residual of each equation, MSE_R, as well as the discrepancy between the predicted and actual data, MSE_d, during the training process.

$$MSE_{Inv} = MSE_R + MSE_d. \quad [3]$$

Having the model parameters from a set of limited experiments, forward RhiGNet is used to predict the stress response of the material under a number of other flow protocols outside the training process, using the constitutive model without any data. One can argue that the forward RhiGNets are alternative ordinary differential equation (ODE)/partial differential equation solvers based on the graph model of TensorFlow, where inputs are correlated directly to the predictions using the constitutive equations and the initial conditions to the problem of interest instead of numerically solving those differential equations. These inputs and their corresponding predictions are used to calculate the residual of the constitutive model, which is to be minimized. Only then can one ensure that the training process is informed by physical intuition. This residual is calculated based on Eq. **4** using the residual of each equation, MSE_R, as well as the discrepancy between the predicted and actual initial/boundary conditions, MSE_{BIC}.

$$MSE_{Dir} = MSE_R + MSE_{BIC}. \quad [4]$$

Once a full predictive mapping of rheological behavior of the fluid in different protocols is made with RhiGNets, these maps can be used as the low-fidelity data for an observational bias method, referred to here as multifidelity RhiGNets (MF-RhiGNets). These MF-RhiGNets predict the precise rheological response of the material to an imposed deformation, allowing them to be used as a digital twin to the rheometer. For each protocol, a number of new experimental measurements are provided as the high-fidelity data, with a much larger map of the RhiGNet-generated low-fidelity predictions. While the low-fidelity data do not accurately predict the rheology, they provide the trends and the general behavior required for optimizing the digital rheometer twin, MF-RhiGNet. While there are several approaches for multifidelity modeling with different levels of complexities (32), we construct the relation between the low- and high-fidelity data through a general expression based on deep NNs. This general form can be expressed as Eq. **5**, in which $\mathcal{G}(.)$ is a general combination of low-fidelity data, y_{LF}, and inputs of the problem at hand, (x). Such a general combination can be decomposed into a linear and a nonlinear part as shown in Eq. **5**.

$$y_{HF} = \mathcal{G}(y_{LF}, x) = \mathcal{G}_l(y_{LF}, x) + \mathcal{G}_{nl}(y_{LF}, x). \quad [5]$$

The training process in the MF-RhiGNets framework is performed by minimizing a loss function defined according to Eq. **6**. In this equation, $MSE_{y_{HF}}$ and $MSE_{y_{LF}}$ are deviations of predicted and actual data for high- and low-fidelity data, respectively. Additionally, w_i is the weight function, and λ is $\mathbb{L}_2$ regularization rates for weight functions to prevent overfitting (33). This multifidelity modeling can therefore be used to increase the accuracy and efficiency of predictions made by NNs (13, 34–36).

$$MSE = MSE_{y_{HF}} + MSE_{y_{LF}} + \lambda \sum w_i^2. \quad [6]$$

We show, in Fig. 1, a schematic view of how RhiGNets and MF-RhiGNets are devised and employed to create a digital rheometer twin that leverages hybrid observational and inductive biases to embed the essential physics into the NNs. The NNs' architecture has a substantial impact on the accuracy of the predictions as well as the algorithm's performance. The number of layers in the MF-RhiGNets architecture, also known as network width, and the number of neurons per layer, also known as network depth, can both affect the accuracy. In this study, we use the relative absolute error as the measure of accuracy to investigate and optimize the role of network hyperparameters and settings. The depth of the NNs was changed from one to eight layers, and the width was changed from 5 to 200 neurons per layer. Widths ranging between 10 and 25, and depths ranging between two and four, are found to yield the best levels of accuracy while avoiding overfitting. Furthermore, the generation of low-fidelity data will increase the total number of data needed to properly train a network. The number of low-fidelity data are chosen in a way that the RAE is not dependent on the number of data. Another parameter that changes the accuracy of multifidelity prediction is the ratio between the number of low- and high-fidelity data points used in the training process. We have shown previously (13) that this ratio can be optimized to ensure efficiency of the platform without compromising the accuracy. Here, a thorough examination of the low-/high-fidelity data size ratio in each stage was conducted, and a range was chosen to ensure the independence of the prediction from the number of low-fidelity data. The loss function is optimized using a combination of Adam optimizer with a learning rate of 1e-3 and limited-memory Broyden-Fletcher-Goldfarb-Shanno algorithm method together with Xavier's initialization method, while the hyperbolic tangent function is employed as the activation function where appropriate.

Results and Discussion

Our ultimate goal is to develop reliable and accurate ML frameworks as metaconstitutive descriptions for effective and accurate rheological modeling. To achieve this goal, we first present the predictions made using RhiGNets to recover the stress response of a complex fluid in several flow protocols. Using inverse RhiGNets, the characteristics and properties of the material in terms of constitutive model parameters are recovered using limited data from simple experiments. In the first step, we use three instances of steady shear start-up to recover all nine parameters of the MIKH model described in Eq. **2**. Conventionally, tens of experimental protocols at different rates are used to recover these parameters. The thixotropic nature of the fluid under investigation implies that different rest times after a rejuvenating preshear the sample lead to different microstructural states at the inception of the flow. Thus, we choose three different rest times of 100, 300, and 500 s prior to start-up of flow at constant deformation rates of $\dot{\gamma} = 1, 10$, and $56.2\ s^{-1}$, respectively. It is worth mentioning that there are no constraints used for parameter recovery of the model in the inverse

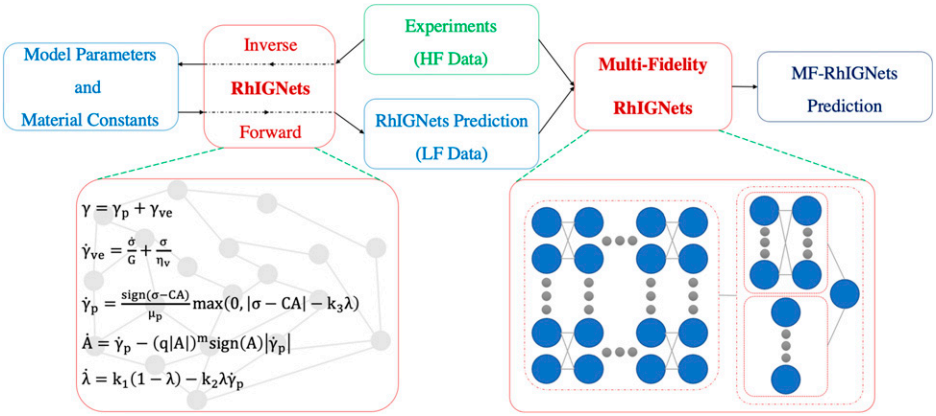

Fig. 1. Schematic view of the digital rheometer twin construction: a hybrid RhiGNets (inductive bias) and MF-RhiGNets (observational bias) platform for accurate rheological predictions. The RhiGNets framework is based on the graph mode of TensorFlow, including MIKH constitutive equations to guide the training process. Limited experimental data are fed to the inverse framework of RhiGNets to acquire material constants and model parameters, followed by forward RhiGNets for preliminary predictions of different flow protocols. Thereupon, a combination of RhiGNet predictions and experimental data is fed to MF-RhiGNets to make digital measurements of unseen flow protocols.

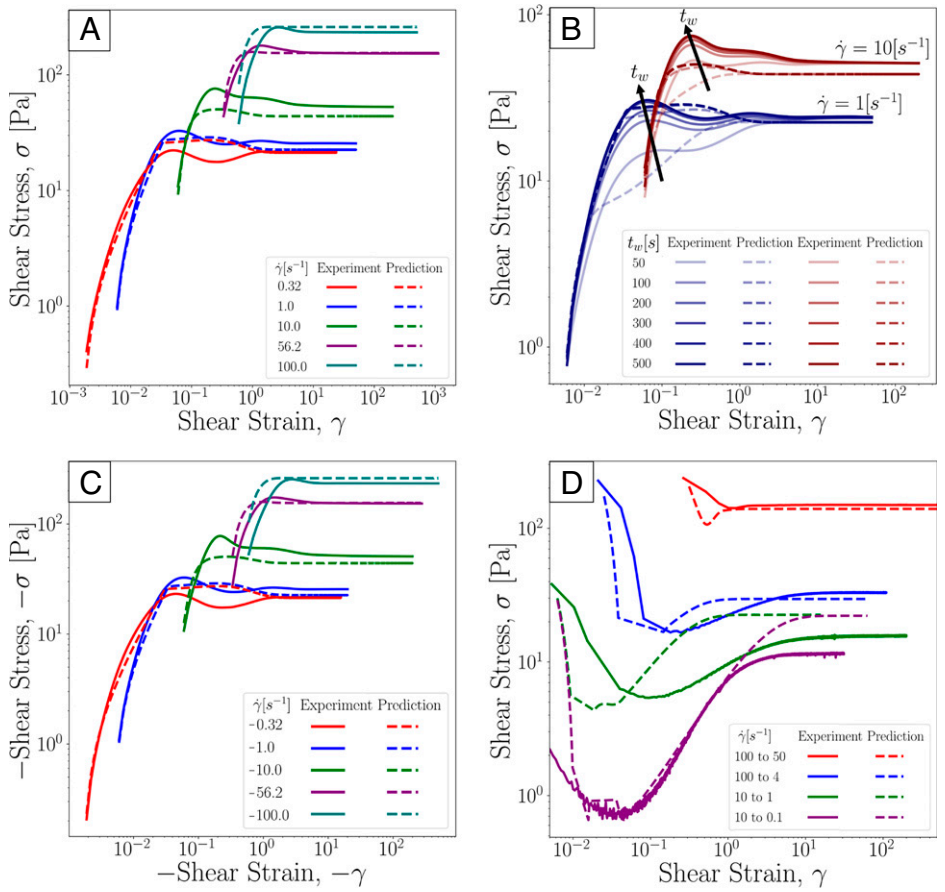

Fig. 2. RhiGNets prediction of (*A*) shear start-up, (*B*) various shelving times, (*C*) flow reversal, and (*D*) stress jump flow protocols for applied shear rates of $O(0.1)$ to $O(100)$.

framework, except some physical ones, such as nonnegative value for elastic modulus. Results from two of these three experiments are plotted in Fig. 2*B*, showing different stress overshoots and long time responses. The recovered material parameters from the inverse RhiGNet for the MIKH model are: $G = 920$ Pa, $\eta_v = 1{,}000$ Pa · s, $\mu_p = 2.4$ Pa · s, $k_1 = 0.02$ 1/s, $k_2 = 3.0$, $k_3 = 25$ Pa, $C = 100$ Pa, $q = 5$, and $m = 1$. A relatively long thixotropic time constant ($1/k1 = 50$ s), and a saturating, and a saturating back stress of $C/q = 20$ Pa in the same range as the static yield stress, $k_3 = 25$ Pa, further suggest a complex rheological response.

Having the material constants for the MIKH parameter, RhiGNet is then used to predict the stress response of the gel under a series of different flow protocols and deformation rates. To this end, start-up of flow at various shear rates and rest times prior to shear, flow reversal, stress jump, and oscillatory shear rates covering a full range of small to large magnitudes are performed and compared against the RhiGNet predictions. Figs. 2 and 3 represent the comparison between the experimentally measured stress response of the fumed silica gel to these flow protocols and the predictions made by RhiGNet based on model parameters recovered from the three initial steady shear start-up experiments. In Fig. 2*A*, shear stress responses of the fluid to start-up of flow experiments with a wide range of shear rates from $\dot{\gamma} = 0.1$ [s^{-1}] to 100 [s^{-1}] are shown after 500 s of rest prior to the inception of flow, qualitatively tracked through the RhiGNet predictions. The results clearly show that the predictions are valid well beyond the range of training data, as the upper and lower limits of shear rates predicted were not used in the recovery of material constants. Furthermore, for the same shear rates applied, RhiGNet can predict the role of rest time from 50 s to 500 s on the stress overshoot and long time stress response of the material as shown in Fig. 2*B* for applied shear rates of $\dot{\gamma} = 1$ and 10 s^{-1}. Flow reversal experiments, in which the applied deformation rate is reversed in sign instantaneously, are also shown in Fig. 2*C*, with stresses and deformation rates shown with a negative sign. Trends similar to the start-up of flow experiments are observed in these measurements where the RhiGNet predictions qualitatively describe the rheology measured experimentally.

Another flow protocol that is commonly used to characterize the thixotropic behavior of a complex fluid is the stress jump experiment, in which the deformation rate is abruptly changed, having already reached stable flow conditions. The evolution of the shear stress is monitored from the time the shear rate was changed. Fig. 2*D* shows the experimental and RhiGNet predictions for the time-dependent stress response from an experiment in which the rate is jumped from $\dot{\gamma} = 100$ and 10 s^{-1} to lower deformation rates. One should note that the accuracy of RhiGNet has its footing in the constitutive model that is chosen to represent the fluid under investigation. As such, and since the IKH model itself does not recover the stress jump experiments accurately, observed deviations are rather expected. Here, rather significant deviations are observed at very short times and small strains, with a very good agreement being observed at longer times and larger strains. Experimentally, the rheometer takes a short but finite amount of time to change the rate, as opposed to an ideal step function. As long as the interval over which the rate is changed is smaller than any material timescale, this finite duration should have minimal effect.

Oscillatory shearing is one of the most informative and commonly used flow protocols for characterizing complex fluids. This protocol allows the user to select the timescale and the strength of flow independently through tuning of the frequency and the

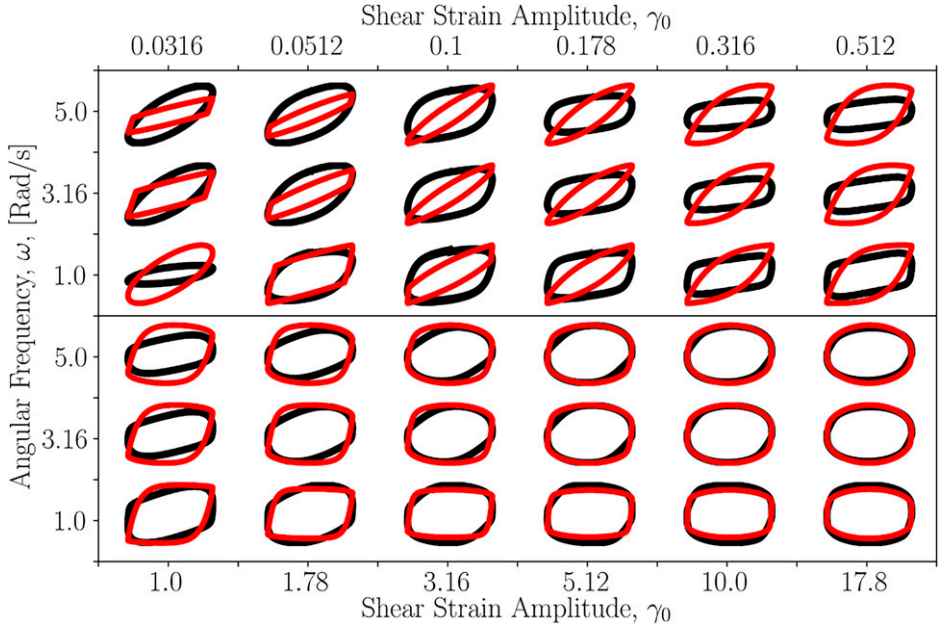

Fig. 3. RhiGNets prediction for oscillatory applied shear strain at three different frequencies and various strain amplitudes.

amplitude and can thus be used to probe a wide range of behaviors. Fig. 3 presents the map of oscillatory shear flow predictions for a wide range of amplitudes from $O(0.01)$ to $O(10)$ and three different frequencies, measured experimentally and also digitally with RhiGNets using the same material parameters recovered from the three initial start-up experiments. The stress response is predominantly elastic at small strain amplitudes, and larger amplitudes elicit nonlinear viscoelastic and elastoviscoplastic responses. While the general trends observed here seem to be appropriately predicted by RhiGNet, large deviations are observed particularly at small and medium amplitudes.

Results presented in Figs 2 and 3 clearly show a qualitative agreement between the experimental data and the prediction made by RhiGNet. There are, however, clear departures from the experimentally measured values that may result from having chosen a constitutive relation that doesn't match the correct physics or poor mapping of the model parameters. Most constitutive models are developed for ideal materials or behaviors that do not lend themselves well to more-complex responses. For example, it is common to assume the existence of an ideal thixotropic and viscoelastic behavior, while real complex fluids such as the one investigated here are believed to have multiple length scales and timescales associated with their microstructural evolution under flow. The state of the microstructure in these gels is best described as being an arrested disordered fractal that spans the sample. Thus, an ideal method of choice to describe and model the rheology is to initially perform a set of experiments to provide a basic understanding of their rheological behavior, followed by refinement through additional experimentation.

Metamodeling frameworks that can learn and evolve with additional experimentation, and which are founded in the fundamental rheological constitutive models, can provide a leap forward in accurate modeling of complex fluids. The main advantage is that, with sufficient training, these metamodels can digitally measure the rheological response of the material, as opposed to qualitatively describing a certain behavior. Here, we implement a multifidelity method to combine the RhiGNet predictions with additional experimental data, and quantitatively describe complex flow behavior of the fumed silica gels. We use the preliminary predictions made by the RhiGNet framework as our low-fidelity data, as these data are generated by the constitutive model. Additional experimental measurements are then included as the high-fidelity data that describe the behavior in the flow protocol under question. For instance, oscillatory shear measurements can be provided as additional training data if the small- or large-amplitude oscillatory shear predictions are sought. In other words, MF-RhiGNets leverage the abundance of low-fidelity data made by RhiGNets, and can learn the accuracy of limited high-fidelity experimental data on the go. As an example, Fig. 4 shows the comparison between MF-RhiGNet predictions for the oscillatory shear strain protocol with the experimental data. These predictions are made by using their respective low-fidelity data generated by RhiGNets, which are presented as red lines in Fig. 3, combined with three additional oscillatory shear experiments. Overall, for each frequency of interest, three experimental measurements are sufficient to enable quantitatively accurate predictions. As clearly shown in Fig. 4, MF-RhiGNet is now capable of predicting the rheology to a sufficiently high degree that it can be regarded as a digital measurement.

All MF-RhiGNets and RhiGNets predictions in Figs. 2–4 have been made using the three sets of experimental start-up of flow data to recover the material parameters. The effect that the choice of the initial flow protocol has on the final predictions is unclear. Here, we seek to interrogate the robustness of the methodology with respect to the type of data that are made available in the first step. To do so, different oscillatory shear experiments that include the initial transient response and the steady alternating state at a frequency of 1 rad/s are used by the inverse RhiGNet. The recovered parameters are presented in Table 1. It should be noted that the parameter m is set to be 1.0 in this table, as it only shows the temperature sensitivity of the material, not the focus of the current study. The values of the viscosities η_v and μ_p, elastic modulus, G, static yield stress, k_3, and the dynamic yield stress, C/q, are found to be consistent regardless of the experiments used in their recovery, and within a reasonable range for all trained systems but the ones with only three sets of steady-state oscillatory shear measurements. The two time constants for the time evolution of microstructure, k_1 and k_2, are consistently recovered to be zero when steady-state data are used for training. This is expected, as the steady state is devoid of transience by

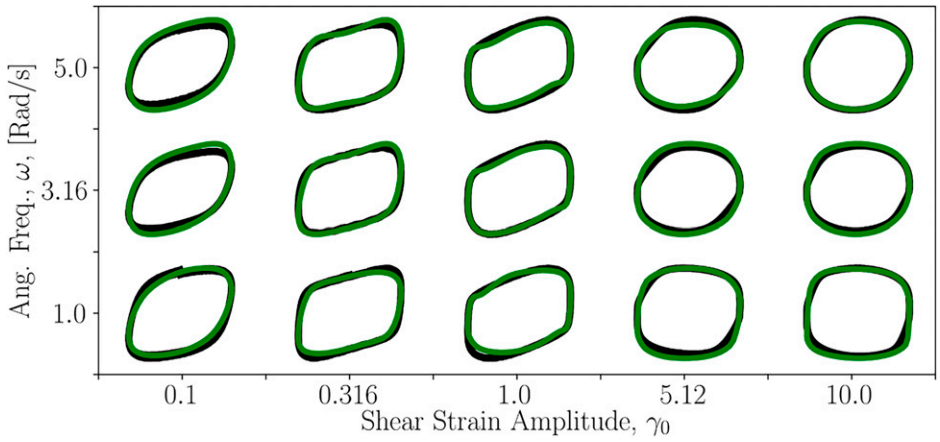

Fig. 4. MF-RhiGNets predictions and experimental measurements for oscillatory shear protocols with three different frequencies and various strain amplitudes. Ang. Freq., angular frequency.

definition, and the microstructure parameters can be recovered analytically. It is also clear, from large deviations in steady-state training sets with three measurements, that at least four sets of measurements are required to recover the material parameters. The results in Table 1 clearly show that the material parameters found by the NN are significantly affected by the choice of initial experiment used in their recovery. This could be because complex constitutive equations such as MIKH, with nine different model parameters, do not necessarily have a unique solution for a given stress response. In other words, different combinations of these model parameters could recover similar rheological behaviors. Another reason that the material parameters are affected by the choice of initial experiment used in their recovery is that not all components of a constitutive model are necessary to recover different flow protocols. That is, some parameters lose their significance in particular experiments. The parts of the models that describe transience will never be probed by steady-state experiments.

While material constants that are recovered from an initial set of experiments vary by changing the protocols used in the experiment, the ultimate goal remains to be obtaining an accurate prediction of rheological features of a complex system. The robustness of the digital rheometer twin lies in its capacity to predict accurate rheological behavior, and not in the values of the parameters corresponding to a particular model. Thus, the predictions are tested against experimental data that MF-RhiGNet has never been exposed to. For this purpose, we choose a stress–growth experiment, using the model parameters recovered from oscillatory shear data. Predictions are shown in Fig. 5. Here, two different sets of MIKH parameters acquired from shear strain amplitude flow protocols shown in Table 1 are used to generate the low-fidelity data and to predict start-up of shear flow at $\dot{\gamma} = 10\ s^{-1}$. Despite the significant differences in the parameters that are used to generate the low-fidelity data, both of these predictions closely track the rheological behavior of the gel in both the transient and the steady-state conditions. One should note that increasing the number of available experimental data during the model parameter recovery step will always result in a more confident retrieval of those parameters. As such, the solution of a complex set of ODEs to one simple applied kinematic may very well not be unique. Nonetheless, it is clear that, even with model parameters that roughly describe the observed experimental measurements, a multifidelity approach will always result in accurate predictions being made for unobserved kinematics.

Conclusion

For many decades, efforts have been made to develop phenomenological and empirical models that describe the rate- and time-dependent rheology of complex fluids. These models have brought valuable insight into the physical underpinnings of the fluids' macroscopic behavior in different flow regimes. However, these models have limited ability to precisely predict the rheological features of real nonideal complex fluids. Here, we have built upon these fundamental physical understandings and leveraged data-driven approaches to introduce an adaptable and comprehensive algorithm that can be used as a digital rheometer. We showed that the RhiGNet platform is capable of learning the hidden rheology of a complex fluid from a very limited number of experiments performed. Note that, alternatively, one can devise rheology-informed NNs to construct new functional forms of the constitutive equations. However, here we denote "hidden rheology" as the rich rheological response of a naturally complex fluid (such as one studied here) that cannot be trivially discovered from a simple applied kinematic such as stress growth

Table 1. Predicted IKH parameters using RhiGNet framework

ID no.	Flow protocol	No. of experiments	G (Pa)	η_v (Pa · s)	μ_p (Pa · s)	k_1 (1/s)	k_2	k_3 (Pa)	C (Pa)	q	m
1	Start-up flow	3	920	1,000	2.4	0.02	3.0	25	100	5.0	1.0
2	Start-up flow	3	800	1,060	2.2	0.04	10.0	45	560	20	1.0
3	Start-up flow	3	820	1,000	1.3	0.01	5.3	43	56	2.5	1.0
4	Transient oscillatory	3	920	987	4.6	0.0	0.03	7.6	33	3.9	1.0
5	Transient oscillatory	3	875	763	3.6	0.0	4.0	8.4	160	11.5	1.0
6	Transient oscillatory	4	1,030	585	4.3	0.0	36	10.6	520	54	1.0
7	Transient oscillatory	4	875	950	4.9	0.0	0.02	7.7	30	3.5	1.0
8	Steady-state oscillatory	3	410	180	4.0	0.0	0.0	8.0	31	4.1	1.0
9	Steady-state oscillatory	3	100	890	3.6	0.0	0.0	5.0	100	10.0	1.0
10	Steady-state oscillatory	4	870	950	4.3	0.0	0.0	5.3	51	10.0	1.0
11	Steady-state oscillatory	4	910	980	4.6	0.0	0.0	7.0	23.6	2.9	1.0

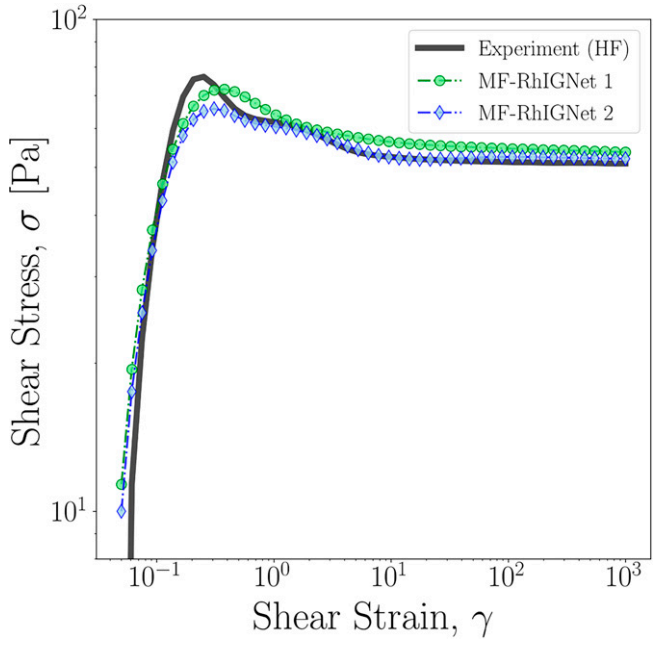

Fig. 5. Prediction of start-up of a flow at shear rate of 10 s^{-1} using two sets of low-fidelity data.

experiments. Once this hidden rheology is learned, predictions of the rheological behavior can be made for flow protocols that have not been observed by the NN, with a qualitative agreement between the predictions and the experimental measurements. More importantly, these predictions can be made almost instantly and can be used as low-fidelity data for the training of MF-RhiGNets. Combining the power of informing the NNs through observational biases and inductive biases, these MF-RhiGNets then can make predictions that quantitatively agree with experiments. These digital measurements can be made using a handful of experiments to characterize a truly complex rheological feature, after which experimentation can be replaced by the digital rheometer, with predictions made at no cost. We also showed that these digital rheometers can learn the hidden rheology through inverse RhiGNets and can therefore be reliably and robustly used regardless of the choice of experimental data employed in their training process. Similar to other digital twins, the accuracy of these digital rheometers increases with additional experiments performed, and, upon reaching an acceptable accuracy, the physical rheometer twin is no longer required for characterization of the fluid. Additionally, the physical rheometer will be prone to experimentation artifacts such as edge fracture of the sample at high shear rates, while the digital rheometer can potentially still function, since the main constitutive equations remain valid regardless of the range of deformation rate applied. This should help in theoretical developments and studies of empirical rule such as Cox–Merz which are generally affected by such limitations. This offers a robust framework for using data-driven and ML algorithms as the next generation of constitutive models with unprecedented efficiency and accuracy. While a particular complex fluid, a fumed silica gel, and a constitutive model, MIKH, have been used in this study, the methodology can be generally applied to all complex fluids and models. Nonetheless, and since the basis of these predictions are founded in the governing constitutive equation describing the observed experiments, extreme caution should be taken in the choice of these physical laws. In other words, limitations of the underlying physical models carry over to the NN predictions, and thus it is of utmost importance to embed constitutive relations that are rigorously derived and are consistent for different applied kinematics and stresses.

Data Availability. All study data presented in the manuscript are available in the Mendeley Data repository, https://doi.org/10.17632/pm98pzpvv9.1 (37).

ACKNOWLEDGMENTS. M.M. and S.J. acknowledge support by Northeastern University's Spark Fund program. This material is based on work supported by NSF Grant 1847389, which K.A.K. and S.A.R. acknowledge.

1. D. Qi, A. J. Majda, Using machine learning to predict extreme events in complex systems. *Proc. Natl. Acad. Sci. U.S.A.* **117**, 52–59 (2020).
2. J. Z. Kim, Z. Lu, E. Nozari, G. J. Pappas, D. S. Bassett, Teaching recurrent neural networks to infer global temporal structure from local examples. *Nat. Mach. Intell.* **3**, 316–323 (2021).
3. E. D. Gennatas *et al.*, Expert-augmented machine learning. *Proc. Natl. Acad. Sci. U.S.A.* **117**, 4571–4577 (2020).
4. L. E. Suárez, B. A. Richards, G. Lajoie, B. Misic, Learning function from structure in neuromorphic networks. *Nat. Mach. Intell.* **3**, 771–786 (2021).
5. M. Raissi, P. Perdikaris, G. E. Karniadakis, Physics-informed neural networks: A deep learning framework for solving forward and inverse problems involving nonlinear partial differential equations. *J. Comput. Phys.* **378**, 686–707 (2019).
6. G. E. Karniadakis *et al.*, Physics-informed machine learning. *Nat. Rev. Phys* **3**, 422–440 (2021).
7. T. Poggio, H. Mhaskar, L. Rosasco, B. Miranda, Q. Liao, Why and when can deep-but not shallow-networks avoid the curse of dimensionality: A review. *Int. J. Autom. Comput* **14**, 503–519 (2017).
8. F. Sahli Costabal, Y. Yang, P. Perdikaris, D. E. Hurtado, E. Kuhl, Physics-informed neural networks for cardiac activation mapping. *Front. Phys.*, **8**, 10.3389/fphy.2020.0042 (2020).
9. X. I. A. Yang, S. Zafar, J. X. Wang, H. Xiao, Predictive large-eddy-simulation wall modeling via physics-informed neural networks. *Phys. Rev. Fluids* **4**, 034602 (2019).
10. X. Jin, S. Cai, H. Li, G. E. Karniadakis, NSFnets (Navier-Stokes flow nets): Physics-informed neural networks for the incompressible Navier-Stokes equations. *J. Comput. Phys.* **426**, 109951 (2021).
11. J. X. Wang, J. L. Wu, H. Xiao, Physics-informed machine learning approach for reconstructing Reynolds stress modeling discrepancies based on DNS data. *Phys. Rev. Fluids* **2**, 034603 (2017).
12. X. Jia *et al.*, Physics-guided machine learning for scientific discovery: An application in simulating lake temperature profiles. *ACM/IMS Trans. Data Sci.* **2**, 20 (2021).
13. M. Mahmoudabadbozchelou *et al.*, Data-driven physics-informed constitutive metamodeling of complex fluids: A multifidelity neural network (MFNN) framework. *J. Rheol. (N.Y.)* **65**, 179–198 (2021).
14. M. Mahmoudabadbozchelou, S. Jamali, Rheology-Informed Neural Networks (RhINNs) for forward and inverse metamodelling of complex fluids. *Sci. Rep.* **11**, 12015 (2021).
15. M. Mahmoudabadbozchelou, G. E. Karniadakis, S. Jamali, nn-PINNs: Non-Newtonian physics-informed neural networks for complex fluid modeling. *Soft Matter* **18**, 172–185 (2021).
16. K. Dullaert, J. Mewis, A model system for thixotropy studies. *Rheol. Acta* **45**, 23–32 (2005).
17. Y. Wei, M. J. Solomon, R. G. Larson, Quantitative nonlinear thixotropic model with stretched exponential response in transient shear flows. *J. Rheol. (N.Y.)* **60**, 1301 (2016).
18. J. Choi, S. A. Rogers, Optimal conditions for pre-shearing thixotropic or aging soft materials. *Rheol. Acta* **59**, 921–934 (2020).
19. R. G. Larson, Constitutive equations for thixotropic fluids. *J. Rheol. (N.Y.)* **59**, 595–611 (2015).
20. Y. Wei, M. J. Solomon, R. G. Larson, A multimode structural kinetics constitutive equation for the transient rheology of thixotropic elasto-viscoplastic fluids. *J. Rheol. (N.Y.)* **62**, 321–342 (2018).
21. R. G. Larson, Y. Wei, A review of thixotropy and its rheological modeling. *J. Rheol. (N.Y.)* **63**, 477–501 (2019).
22. C. J. Dimitriou, G. H. McKinley, A comprehensive constitutive law for waxy crude oil: A thixotropic yield stress fluid. *Soft Matter* **10**, 6619–6644 (2014).
23. M. Geri, R. Venkatesan, K. Sambath, G. H. McKinley, Thermokinematic memory and the thixotropic elasto-viscoplasticity of waxy crude oils. *J. Rheol. (N.Y.)* **61**, 427–454 (2017).
24. S. L. Brunton, B. R. Noack, P. Koumoutsakos, Machine learning for fluid mechanics. *Annu. Rev. Fluid Mech.* **52**, 477–508 (2020).
25. X. Meng, G. E. Karniadakis, A composite neural network that learns from multi-fidelity data: Application to function approximation and inverse PDE problems. *J. Comput. Phys.* **401**, 109020 (2020).
26. P. Pant, R. Doshi, P. Bahl, A. Barati Farimani, Deep learning for reduced order modelling and efficient temporal evolution of fluid simulations. *Phys. Fluids* **33**, 107101 (2021).
27. M. Abbaszadeh *et al.*, A reduced-order variational multiscale interpolating element free Galerkin technique based on proper orthogonal decomposition for solving Navier–Stokes equations coupled with a heat transfer equation: Nonstationary incompressible Boussinesq equations. *J. Comput. Phys.* **426**, 109875 (2021).
28. A. T. Mohan, N. Lubbers, D. Livescu, M. Chertkov, Embedding hard physical constraints in neural network coarse-graining of 3D turbulence. arXiv [Preprint] (2020). https://arxiv.org/abs/2002.00021v2 (Accessed 15 February 2020).
29. M. Raissi, A. Yazdani, G. E. Karniadakis, Hidden fluid mechanics: Learning velocity and pressure fields from flow visualizations. *Science* **367**, 1026–1030 (2020).
30. L. Lu *et al.*, Physics-informed neural networks with hard constraints for inverse design. *SIAM J. Sci. Comput.* **43**, 10.1137/21M1397908 (2021).
31. K. Xu, E. Darve, ADCME: Learning spatially-varying physical fields using deep neural networks. arXiv [Preprint] (2020). https://doi.org/10.48550/arXiv.2011.11955 (Accessed 24 November 2020).
32. M. Giselle Fernández-Godino, C. Park, N. H. Kim, R. T. Haftka, Issues in deciding whether to use multifidelity surrogates. *AIAA J.* **57**, 2039–2054 (2019).
33. D. Zhang, L. Lu, L. Guo, G. E. Karniadakis, Quantifying total uncertainty in physics-informed neural networks for solving forward and inverse stochastic problems. *J. Comput. Phys.* **397**, 108850 (2019).
34. C. Pan *et al.*, Increasing efficiency and accuracy of magnetic interaction calculations in colloidal simulation through machine learning. *J. Colloid Interface Sci.* **611**, 29–38 (2022).
35. M. Raissi, G. Karniadakis, Deep multi-fidelity Gaussian processes. arXiv [Preprint] (2016). https://doi.org/10.48550/arXiv.1604.07484 (Accessed 26 April 2016).
36. D. Liu, Y. Wang, Multi-fidelity physics-constrained neural network and its application in materials modeling. *J. Mech. Des.* **141**, 121403 (2019).
37. M. Mahmoudabadbozchelou, K. M. Kamani, S. A. Rogers, S. Jamali, PNAS - Digital Rheometer Twin. Mendeley Data. https://doi.org/10.17632/pm98pzpvv9.1. Deposited 14 April 2022.